Project Progress Report: Quantum Graph Approaches to Molecular Vibrations — Second Semester

Király Bálint Dániel

May 17, 2026

1 Introduction

The first semester established the quantum graph model of CH_5^+ (protonated methane), following the framework of Rawlinson, Fábri, and Császár [5]. The central result was the spectral relation $E = \arccos^2(\lambda/k) \,/\, (2l^2)$, which converts adjacency eigenvalues of the Γ_{60} graph into vibrational energy levels, together with an initial SymPy-based implementation of the `QuantumGraph` class. Three directions were identified for further work: a rigorous treatment of vertex boundary conditions, extension to other fluxional molecules, and generalization of the spectral relation to non-regular graphs. In parallel, my supervisor A. G. Császár is preparing a paper on quantum graph models of fluxional molecules; throughout this report it is referred to as *the manuscript*, and one of the main activities of the second semester was contributing new and revised content to several of its sections.

The second semester made progress on all three fronts, both on the theoretical and on the practical side. On the theoretical side, Berkolaiko and Kuchment [2] were acquired as the primary mathematical reference; five vertex boundary condition types were formalized; and a new closed-form pairing identity was derived for the energy levels of any k-regular bipartite quantum graph with uniform edge length. The corresponding content was written into the manuscript. On the practical side, the verified construction of the Γ_{120} and Γ_{60} graphs of CH_5^+ was implemented, with the spectrum of Γ_{60} checked against the published values of Rawlinson et al. [5]; a dual-solver physics engine was developed, combining a fast adjacency-based solver for regular graphs with a general Bond Scattering Matrix solver for arbitrary graphs; and a full Flask-based web calculator was built on top of the engine, providing an interactive graph editor, energy-level computation, secular-function scans, wavefunction visualization, and wavepacket dynamics. Extension to other fluxional molecules was deferred in favour of deepening the treatment of CH_5^+, including the beginning of a study of the rovibrational model of Rawlinson (2019) [4], which frames the primary research direction for the third semester.

2 Theoretical Study

2.1 Atkins, *Physical Chemistry*, Chapters 8–9

The second semester began with a systematic reading of Atkins, *Physical Chemistry* [1], to consolidate the physical foundations of the model. Chapter 8 was studied in depth: wave–particle duality, the time-independent Schrödinger equation, the Born probabilistic interpretation of the wavefunction, and the Heisenberg uncertainty principle. These concepts are directly relevant to the quantum graph setting, where the wavefunction $\psi_j(x)$ on each edge j is a solution of the one-dimensional Schrödinger equation and is interpreted as a probability amplitude.

Chapter 9 was studied with emphasis on the problems most directly connected to the quantum graph model. The particle in a one- and two-dimensional box provided a clean exact-solvable analogue of a graph edge with Dirichlet endpoint conditions, and made the quantization mechanism (boundary conditions selecting a discrete set of energies from a continuous family of solutions of

the Schrödinger equation) concrete. The discussion of vibrational energy levels for the harmonic oscillator gave physical meaning to the energy units (cm^{-1}) used throughout the project. The particle on a ring and the particle on a sphere were studied as well, partly as further examples of exactly solvable quantum-mechanical models with non-trivial boundary conditions, and partly as preparation for the rovibrational extension, in which angular degrees of freedom enter the problem explicitly. These models, however, are not themselves quantum graphs in the sense used throughout this project, as their configuration spaces are intrinsically curved (a circle embedded in $\mathbb{R}^2$ and the surface of a sphere, respectively) rather than piecewise-linear unions of one-dimensional edges. Perturbation theory was encountered in this chapter but was not studied in depth, as it does not enter the current implementation.

2.2 *Introduction to Quantum Graphs* by Berkolaiko and Kuchment (2013)

The book *Introduction to Quantum Graphs* by Berkolaiko and Kuchment [2] was acquired as the primary mathematical reference for the project. It covers the theory of metric graphs and quantum graphs systematically: definition of metric graphs, self-adjoint extensions of the Laplacian, vertex conditions, the secular equation and its derivation from the Bond Scattering Matrix formalism, and spectral theory including eigenvalue estimates and trace formulae.

During the second semester, the text served chiefly as the source for the vertex conditions section written into the manuscript. The standard Kirchhoff (Neumann–Kirchhoff) boundary condition, which the implementation uses at all interior vertices, requires both continuity of the wavefunction and the vanishing of the sum of outgoing derivatives:

$$\psi_j(v) = \psi_{j'}(v) \quad \forall\, j, j' \text{ incident at } v, \qquad \sum_{j \sim v} \frac{\mathrm{d}\psi_j}{\mathrm{d}x_j}(v) = 0. \tag{1}$$

Study of the text is ongoing; the rovibrational and spectral-theory sections remain to be worked through in the third semester.

2.3 Rawlinson (2019) Rovibrational Paper

The paper by Rawlinson [4] (*J. Chem. Phys.* **151**, 164303, 2019) was acquired and partially studied. It extends the quantum graph model from purely vibrational energy levels to rovibrational levels by working with the full Γ_{120} graph and incorporating non-zero total angular momentum J. The Γ_{60} model of the 2021 ChemComm paper [5] is recovered in the $J = 0$ limit.

The rovibrational formalism is understood in principle: the Γ_{120} graph encodes both the vibrational and rotational degrees of freedom of the molecule, and the energy levels are obtained from a generalized secular equation that depends on J. Full assimilation of the technical details — in particular the construction of the J-dependent scattering matrix and the symmetry decomposition under the molecular symmetry group S_5^* — remains in progress. The Rawlinson (2019) paper frames the primary research direction for the third semester.

3 Contributions to the Manuscript

The manuscript introduced in Section 1, currently being prepared for publication by A. G. Császár, presents quantum graph models of fluxional molecules and is intended to systematize the framework introduced in [3, 5]. During the second semester I contributed to it at two confidence levels: contributions that have been completed, verified, and incorporated into the working draft, and contributions that have been written and submitted but are still pending review.

3.1 Completed and Verified Contributions

Several foundational sections were revised for mathematical precision. The definitions of directed and undirected graphs were corrected by fixing an inconsistency in the edge-direction convention; the definitions of finite and infinite graphs were rewritten in set-theoretic language; the distinction between walk and path was clarified and formalized; and the definition of a connected graph was

restated rigorously. These changes affect the opening pages of the graph-theory section and establish clean notation for the rest of the text.

The treatment of the incidence matrix was substantially extended. The unsigned incidence matrix X and the oriented incidence matrix B were introduced with full definitions, and the identity $BB^\top = L^C$ (where L^C is the combinatorial Laplacian) was proved, together with the observation that the identity is independent of the chosen edge orientation. This replaced a placeholder paragraph that had been present in the draft.

Two spectral results were proved. First, the normalized Laplacian eigenvalues were shown to lie in $[0, 2]$ using the Perron–Frobenius theorem applied to the random-walk matrix. Second, the odd-degree theorem was proved — a k-regular graph with odd k must have an even number of vertices — along with its contrapositive; the converse was shown to be false by the counterexample of the 4-cycle C_4, which is 2-regular (even degree) but has four vertices. Minor corrections throughout the manuscript included fixing the units on k_{max} and adding equation labels to unnumbered display equations.

3.2 Contributed, Pending Review

The larger prose contributions are still under review. Section 2.4 was clarified to state that the Hamiltonian $\hat{H}$ acts on $L^2(\Gamma)$ with each edge function f_j belonging to the Sobolev space $H^2(0, L_j)$, providing the proper functional-analytic formulation of the domain.

Section 2.5, on vertex conditions, was written from scratch (approximately 130 lines). It covers all five boundary condition types recognized by Berkolaiko and Kuchment [2]: the δ-type condition (generalized Kirchhoff with coupling constant α_l), vertex Dirichlet conditions (the formal limit $\alpha_l \to \infty$, giving $\psi = 0$ at the vertex), extended δ-type conditions (a trigonometric unification parameterized by $\gamma_l \in [0, \pi/2]$), decoupling conditions (with vertex Dirichlet and vertex Neumann as limiting cases), and δ'-type conditions (in which the roles of function values and derivatives are interchanged relative to the δ case).

A bijection argument for bipartite graphs was written for Section 2: the map $\hat{T} : (v_1, v_2) \mapsto (v_1, -v_2)$, where the vertices are partitioned into the two parts of the bipartite graph, is a bijection between the eigenspaces V_λ and $V_{-\lambda}$ of the adjacency matrix, establishing that positive and negative eigenvalues of equal magnitude always occur with equal multiplicity.

Section 6 was written in full, covering the determination of the number of connected components via the zero-eigenvalue multiplicity of the combinatorial Laplacian L^C, the group-theoretic orbit argument that counts components, and the block-diagonal factorization of the secular equation for disconnected graphs.

The most original result of the semester appears in Section 9. Combining the spectral symmetry of bipartite graphs (which guarantees that λ and $-\lambda$ are always paired) with the spectral relation $E = \arccos^2(\lambda/k) \,/\, (2l^2)$, the following identity was derived for any k-regular bipartite quantum graph with uniform edge length l:

$$\sqrt{E_1} + \sqrt{E_2} = \frac{\pi}{\sqrt{2}\, l}, \tag{2}$$

where E_1 and E_2 are the energies corresponding to eigenvalues $+\lambda$ and $-\lambda$, respectively. The proof is short: starting from $\lambda = k\cos\!\left(\sqrt{2E}\, l\right)$ and using $\cos\!\left(\sqrt{2E_2}\, l\right) = -\cos\!\left(\sqrt{2E_1}\, l\right) = \cos\!\left(\pi - \sqrt{2E_1}\, l\right)$ for the partner eigenvalues, the principal-branch solution gives $\sqrt{2E_2}\, l = \pi - \sqrt{2E_1}\, l$, which rearranges to Eq. (2). Notably, the identity is independent of the vertex degree k. Section 11 received a corollary that all energy ratios in the Γ_{60} model equal unity, which follows directly from Eq. (2) when $E_1 = E_2$ (i.e., when $\lambda = 0$).

4 Practical Implementation

4.1 CH_5^+ Graph Construction

The verified construction of the Γ_{120} and Γ_{60} graphs is implemented in `ch5plus_quantum_graph.py`. The graph Γ_{120} is the Cayley graph of the symmetric group S_5 with respect to a generating set

of three permutations, each corresponding to a physically accessible rearrangement of the five proton labels of CH_5^+. The vertices of Γ_{120} are therefore the $|S_5| = 120$ permutations of the five labels. The three generators are written here in one-line cycle notation (i.e. the tuple $(i_0, i_1, i_2, i_3, i_4)$ denotes the permutation that sends label 0 to i_0, label 1 to i_1, and so on): a clockwise rotation $R_{\mathrm{CW}} = (0, 2, 3, 4, 1)$, the counter-clockwise rotation $R_{\mathrm{CCW}} = R_{\mathrm{CW}}^{-1}$, and a flip FLIP $= (1, 0, 4, 3, 2)$. Each generator defines an edge type: there is an edge between two vertices σ and σ' exactly when $\sigma' = \sigma \cdot g$ for some generator g. Because there are three generators, every vertex has exactly three neighbours, and Γ_{120} is 3-regular on 120 vertices.

The graph Γ_{60} is then obtained from Γ_{120} by contracting all flip edges: since FLIP is an involution, the pairs $\{\sigma, \sigma \cdot \mathrm{FLIP}\}$ are well defined, and each such pair is identified as a single vertex of Γ_{60}. This reduces the vertex count from 120 to 60 and raises the degree from 3 to 4. The resulting 60-vertex, 4-regular graph is bipartite. Its adjacency eigenvalue spectrum was computed and compared against Table 2 of Rawlinson et al. [5]; the match is exact (same eigenvalues, same degeneracies, same ordering). Table 1 gives the first twelve energy levels. The script outputs the adjacency matrices as `A_gamma60.npy`, `A_gamma60.csv`, and `A_gamma60.json` (and equivalently for Γ_{120}).

Table 1: First twelve vibrational energy levels of the Γ_{60} model. The degeneracy g gives the eigenvalue multiplicity. Energies were computed with edge length $l = 0.1322$ (internal units); the $\sim 2.3\,\%$ systematic offset from the reference arises from the use of a trial value of l rather than the supervisor's calibrated value. The spectral structure (degeneracies, ordering, symmetry) is reproduced exactly.

λ	g	Computed E (cm^{-1})	Rawlinson 2021 (cm^{-1})
4.000	1	0.0	0.0
3.236	4	11.3	11.6
2.562	5	21.9	22.5
1.562	5	39.1	40.1
1.236	4	45.2	46.3
1.000	11	49.7	50.9
-1.000	11	95.1	97.4
-1.236	4	101.7	104.1
-1.562	5	111.2	113.9
-2.562	5	146.9	150.4
-3.236	4	180.7	185.1
-4.000	1	282.4	289.2

4.2 Physics Engine

The physics engine is implemented in `quantum_graph.py` (~ 840 lines). The Flask application automatically selects one of two solver paths based on the regularity of the input graph.

Path A, `find_energy_levels_regular`, handles k-regular graphs with uniform edge lengths. It computes the adjacency eigenvalues λ_i of the graph and applies the spectral relation $E = \arccos^2(\lambda/k) \,/\, (2l^2)$ directly. This path is fast and exact for the class of graphs to which it applies.

Path B, `find_energy_levels_general`, handles arbitrary graphs. It constructs the Bond Scattering Matrix $S(k)$, which encodes the Neumann–Kirchhoff boundary conditions at each vertex by expressing outgoing amplitudes as linear combinations of incoming amplitudes. The energy levels are the values of $k^2/2$ at which the secular equation

$$\det\bigl(I - e^{ikL}\, S(k)\bigr) = 0 \tag{3}$$

is satisfied, where L is the diagonal matrix of edge lengths. The zeros are located by scanning k over a grid and bracketing sign changes of the real-valued secular function; this method works for non-regular and non-uniform-edge-length graphs alike.

The graph library includes path graphs, cycle graphs, complete graphs, the Petersen graph (10 vertices, 3-regular), the icosahedral graph (12 vertices, 5-regular), the Desargues graph (20 vertices, 3-

regular), and Γ_{60} (60 vertices, 4-regular bipartite). Supporting functions handle eigenfunction computation (`compute_eigenfunction`), adjacency-spectrum retrieval (`get_adjacency_spectrum`), and graph property queries (`graph_properties`, `is_bipartite`). Two symmetry tables — for S_5^* (14 irreducible representations) and S_4^* — are stored in the module for future symmetry-resolved energy level calculations. Unit conversion routines (`energy_au_to_cm1`, `energy_cm1_to_au`) ensure consistent physical units throughout.

4.3 Web Application

The web application provides a browser-based interface to the physics engine. The stack is a Flask (Python) backend with a vanilla JavaScript frontend requiring no build step; the entry point is `run.py`, which starts a local server at `http://localhost:5050`.

The backend (`app.py`) exposes six REST endpoints. `POST /api/compute` is the main computation endpoint; it receives a graph payload, auto-selects the appropriate solver, and returns energy levels. `POST /api/graph-info` returns graph topology and adjacency spectrum without running the energy solver. `POST /api/secular-scan` evaluates the secular function $\det(I - e^{ikL}S)$ over a specified k range, enabling visualization of zero locations. `POST /api/eigenfunction` returns wavefunction amplitudes on each edge for a specified k value. `POST /api/eigenstates-bulk` returns all eigenstates for wavepacket dynamics computations. `GET /api/builtin-graphs` serves the preset graph metadata to the frontend.

The frontend (`static/js/`) consists of ten JavaScript modules loaded in a fixed dependency order. `graph.js` implements a D3.js force-directed graph editor in which nodes can be dragged, edges added or removed, and individual edge lengths set. `compute.js` triggers the backend and renders the returned energy table in cm^{-1}. `charts.js` draws the energy-level bar chart and the secular-function scan plot using Chart.js. `wavefunction.js` provides a D3-based visualization of the wavefunction $\psi(x)$ along each edge. `dynamics.js` implements wavepacket time evolution using `requestAnimationFrame`. `io.js` handles import and export of graphs in four formats: JSON, adjacency matrix, edge list, and Graph6. `state.js` provides centralized state management, ensuring that the graph payload used for dynamics and eigenfunction computations is always consistent with the last previewed or computed graph, regardless of which interface panel is active. Four built-in presets are available from the preset panel: Petersen, Icosahedral, Desargues, and Γ_{60}.

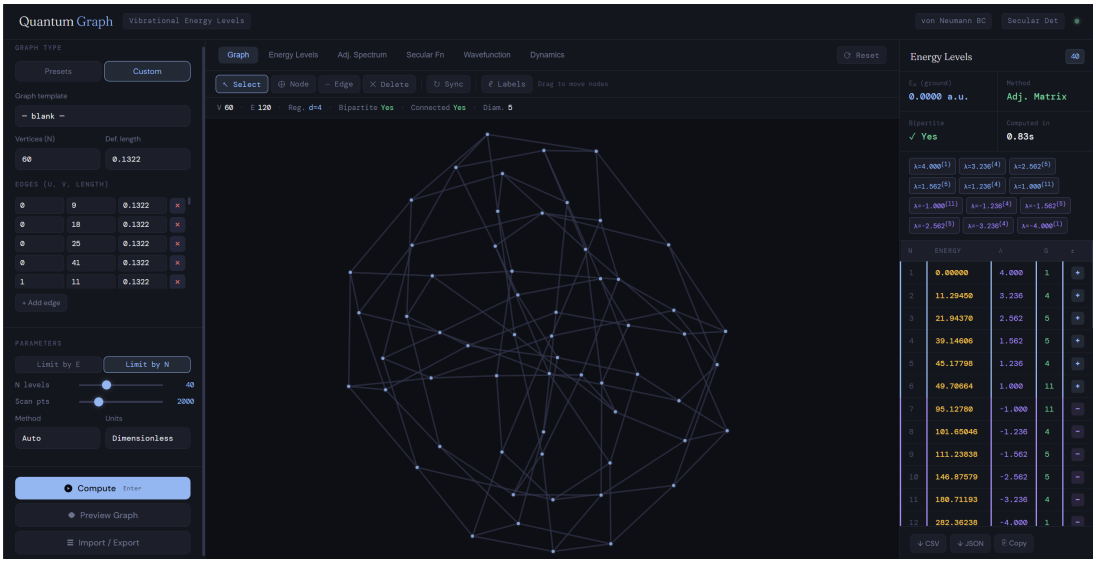

Figure 1: The web-based quantum graph energy level calculator. Left: interactive graph editor (D3.js) showing the Γ_{60} graph. Right: computed vibrational energy levels in cm^{-1}.

4.4 Verification

Three independent checks confirm the correctness of the implementation. First, cross-solver consistency was verified: for all regular preset graphs (Petersen, Icosahedral, Desargues, Γ_{60}), both Path A (regular solver) and Path B (BSM solver) produce identical energy levels, demonstrating that the BSM implementation is correct on the class of graphs for which the exact algebraic result is known.

Second, the bipartite pairing identity (Eq. (2)) was checked numerically against the computed Γ_{60} energy levels. For all six eigenvalue pairs $(\lambda, -\lambda)$, the identity $\sqrt{E_1} + \sqrt{E_2} = \pi/(\sqrt{2}\, l)$ holds to six decimal places. For example, with $l = 0.1322$: $\sqrt{49.707} + \sqrt{95.128} = 16.8036 = \pi/(\sqrt{2} \cdot 0.1322)$. This provides an independent numerical confirmation of the analytical result derived in Section 3.

Third, the adjacency eigenvalue degeneracies for Γ_{60} match the expected S_5^* irreducible representation dimensions exactly, confirming that the graph construction faithfully represents the correct molecular symmetry.

5 Summary and Future Work

The second semester deepened the theoretical foundations on two levels. Atkins, *Physical Chemistry* [1], supplied physical intuition for graph-supported wavefunctions through several exactly solvable model problems, in particular the particle in a box, which is the direct analogue of a single quantum graph edge with Dirichlet endpoint conditions, and the harmonic oscillator, which fixed the energy units used throughout the project. Berkolaiko and Kuchment [2] supplied the rigorous mathematical framework for vertex conditions that was needed for the manuscript. The manuscript itself received substantial new content: precise graph-theoretic definitions, a complete treatment of five vertex boundary condition types, and the derivation of the bipartite pairing identity (Eq. (2)), a closed-form relation between paired energy levels in any k-regular bipartite quantum graph that is independent of the vertex degree. The practical implementation was substantially extended: the Γ_{60} and Γ_{120} graphs were constructed and their spectra verified against the literature, and a full Flask-based web calculator was implemented, providing an interactive graph editor, a dual solver, wavefunction visualization, and wavepacket dynamics.

Three directions are prioritized for the third semester. *First*, and most significant, the rovibrational extension: once the Rawlinson (2019) [4] rovibrational formalism is fully assimilated, the implementation will be extended from the $J = 0$ vibrational-only Γ_{60} model to the full $J > 0$ rovibrational treatment using Γ_{120}. *Second*, the general BSM solver will be applied to other fluxional molecules treated in the manuscript — CH_4^+, $C_2H_7^+$, and bullvalene ($C_{10}H_{10}$) — fulfilling the objective deferred from the first semester. *Third*, the manuscript contributions in Sections 2.5, 6, and 9 require review and possible revision before the manuscript can be submitted.

References

[1] P. Atkins and J. de Paula. *Atkins' Physical Chemistry*. W. H. Freeman and Company, New York, 8th edition, 2006.

[2] Gregory Berkolaiko and Peter Kuchment. *Introduction to Quantum Graphs*, volume 186. American Mathematical Society, 2013.

[3] C. Fábri and A. G. Császár. Vibrational quantum graphs and their application to the quantum dynamics of CH_5^+. *Phys. Chem. Chem. Phys.*, 20:16913–16917, 2018.

[4] J. I. Rawlinson. Quantum graph model for rovibrational states of protonated methane. *J. Chem. Phys.*, 151:164303, 2019.

[5] J. I. Rawlinson, C. Fábri, and A. G. Császár. Exactly solvable 1D model explains the low-energy vibrational level structure of protonated methane. *Chem. Commun.*, 57:4827–4830, 2021.